SparseTag: High-Precision Backscatter Indoor Localization with Sparse RFID Tag Arrays

†Chao Yang, ‡Xuyu Wang, and †Shiwen Mao
†Department of Electrical and Computer Engineering, Auburn University, Auburn, AL 36849-5201, USA
‡Department of Computer Science, California State University, Sacramento, CA 95819-6021, USA
Email: czy0017@auburn.edu, xuyu.wang@csus.edu, smao@ieee.org

***Abstract*—In this paper, we study the problem of utilizing a sparse RFID tag array for backscatter indoor localization. We first theoretically and experimentally validate the feasibility of using RFID tag array for direction of arrival (DOA) estimation. We then present the SparseTag system, which leverages a novel sparse RFID tag array for high-precision backscatter indoor localization. The SparseTag system includes sparse array processing, difference co-array design, DOA estimation using a spatial smoothing based method, and a localization method, while a robust channel selection method based on the RFID tag array is proposed for mitigating the indoor multipath effect. The SparseTag system is implemented with commodity RFID devices. Its superior performance is validated in two different environments with extensive experiments.**

***Index Terms*—RFID; indoor localization; direction of arrival, sparse tag array; difference co-array.**

I. Introduction

With the rapid growth of Internet of Things (IOT), the Radio Frequency Identification (RFID) technology has been regarded as an effective and low-cost solution for many emerging IoT applications [1]–[4]. Existing works on RFID tag localization include received signal strength indication (RSSI) based [5] and phase based [6]–[10] methods. Recently, RFID tag array has drawn increasing attention, which has been used for orientation tracking, 3-Dimensional (3D) reconstruction, and localization. These works mainly leverage the RFID phase information collected using an RFID reader [11]. For example, Tagyro uses a hologram based method to transform phase offset to orientation of the RFID tag array [12], which can track the 3D orientation of passive objects. RF-Wear is developed for orientation estimation with a uniform linear array (ULA), which is used for body-frame tracking [13]. RF-3DScan [14] and 3DLoc [15] utilize a moving antenna for 3D reconstruction and localization, respectively, with an RFID tag array.

A unique challenge for using an RFID tag array is the *mutual coupling* among adjacent tags, which leads to a frequency offset as well as an amplitude offset of the resonance peak [16], [17]. The Trio system aims to take advantage of tag interference for accuracy localization [18]. It leverages two moving tags as reference. When the reference tags are closer to the target tag, the three tags will produce a large interference, which affects the RSSI. Exploiting phase difference information, multiple pairs of tags are used for localization and reader calibration in [19]. This work is based on the hyperbolic based method, and requires solving an optimization problem to achieve high localization accuracy.

Although interesting results have been demonstrated, it is still an open problem to use direction of arrival (DOA) for accurately localizing *static tags*. This is an important problem, since in many RFID applications, tags are not moving. To achieve higher accuracy of angle estimation, more tags should be employed in the tag array. However, the tag density could be very high when multiple tags are placed on a small surface of the object, such as a book or a small package. In such scenarios, the accuracy is heavily influenced by the strong coupling effect. Thus, how to design a suitable tag array under strong mutual coupling for accurately DOA estimation is still a big challenge.

In this paper, we study the problem of applying RFID tag arrays for backscatter indoor localization under mutual coupling and multipath effect. We propose a new sparse RFID tag array design, where tags are not placed at a constant distance from each other. This arrangement can achieve highly accurate localization of static tags with a limited number of tags. We first introduce the measured phase and phase difference information between two tags. We then prove that when the two tags have strong mutual coupling, if they have the same chip and antenna input impedance, the ratio of their equivalent source currents equals to the ratio of their equivalent source voltages. This implies that the phase difference between the two tags is independent to the coupled voltage and the mutual impedance, which provides the underpinning for employing RFID tag arrays for DOA estimation even under mutual coupling. Next, we experimentally demonstrate that for two tags with mutual coupling, the phase from a single tag has large variations, but the phase difference between the two tags is quite stable. This validates the earlier analysis on the independence of phase difference to mutual coupling.

We present the SparseTag system, i.e., a **Sparse** RFID **Tag** array system for high-precision backscatter indoor localization. We first model the sparse array processing for DOA estimation, which is quite different from the traditional MUSIC based method with a ULA [20]. The key is to obtain a new signal vector with a difference co-array, which is a longer array whose antenna locations are not evenly spaced. In addition, we design a new sparse RFID tag array. Our new design has a symmetric structure, which helps to mitigate the mutual coupling effect. We derive its difference co-array and prove several properties, such as its hole-free feature, degrees of free-

978-1-7281-1207-7/19/$31.00 ©2019 IEEE

dom (DOF), and weight function. We analytically show why the proposed sparse RFID tag array can outperform ULA on DOA estimation. Then, we develop a DOA estimation scheme using the difference co-array of the proposed sparse RFID tag array with a spatial smoothing based method. Finally, we provide a localization method based on the two estimated DOAs, where a robust channel selection method is proposed for mitigating the multipath effect. We implement SparseTag with commodity RFID devices and evaluate its performance in two indoor environments, including a computer laboratory and an anechoic chamber, where superior angle estimation and location performance are demonstrated.

The main contributions of this paper are summarized below.

- We theoretically and experimentally validate the feasibility of utilizing an RFID tag array for DOA based indoor localization. To the best of our knowledge, this is the first work to leverage sparse RFID tag array for backscatter indoor localization with no need to move either the tags or the antenna(s).
- We design the SparseTag system, which includes sparse array processing, difference co-array design, DOA estimation using a spatial smoothing based method, and localization method. We propose a new sparse RFID tag array design and analytically prove its superior performance over ULA. Moreover, a robust channel selection method based on the sparse tag array is proposed for mitigating the indoor multipath effect.
- We implement SparseTag with commodity RFID devices and evaluate its performance in two indoor environments, including a computer laboratory and an anechoic chamber. The experimental results verify the effectiveness of the proposed SparseTag system.

In the remainder of this paper, we analyze phase difference and multual coupling in Section II. We present the SparseTag design in Section III and validate its performance in Section IV. Section V summarizes this paper.

II. Phase Difference and Mutual Coupling

A. RFID Phase and Phase Difference

According to FCC regulations, Ultra High Frequency (UHF) RFID readers adopt channel hopping to avoid co-channel interference. In the US, UHF RFID readers operate in the band from 902.5 to 927.5 MHz and hop among 50 different frequencies with 0.2s on each channel. From the RFID reader manual [21], the measured phase φ can be modeled as

$$\varphi = \text{mod}\left(\frac{2\pi 2l}{\lambda} + \alpha_T + \alpha_R + \alpha_{Tag}, 2\pi\right), \quad (1)$$

where l is the tag-reader distance, λ is the wavelength, and α_T, α_R, and α_{Tag} are the phase offsets caused by the transmitter circuit, the receiver circuit, and the tag's reflection characteristics, respectively. When a single tag is used, we find that although the measured phase for a fixed distance over the same frequency is constant, it cannot be directly used for distance estimation because of the phase offsets.

To remove the phase offset, we employ an RFID tag array and measure the phase difference $\Delta\varphi_{1,2}$ between two adjacent tags 1 and 2, i.e.,

$$\Delta\varphi_{1,2} = \text{mod}\left(\frac{2\pi 2l_1}{\lambda} - \frac{2\pi 2l_2}{\lambda} + \alpha_{Tag1} - \alpha_{Tag2}, 2\pi\right), \quad (2)$$

where l_1 and l_2 are the tag-reader distances, and α_{Tag1} and α_{Tag2} are the reflection characteristics from tag 1 and tag 2, respectively. This way, the phase offsets from the transmitter and receiver circuits can be removed. Moreover, for a far-field environment, the incoming wave is like a plane wave. Thus, the phase difference $\Delta\varphi_{1,2}$ between tag 1 and tag 2 can be used for estimating the unique DOA when the distance between the two tags is less than $\frac{\lambda}{4}$ (because of the round-trip distance) [19]. For accurate DOA estimation, we will focus on the effect of $(\alpha_{Tag1} - \alpha_{Tag2})$ in the rest of this section.

B. Mutual Coupling of RFID Tags

When multiple RFID tags are placed close to each other, the mutual coupling between their antennas becomes a significant factor affecting the system performance. Consider the parallel linear dipoles of two tags. When their distance becomes smaller, the mutual coupling effect will be stronger. The coupling effect will change the characteristics of tag antennas, thus influencing the measured phase values and the received power. We next analyze the impact of mutual coupling on measured phase difference and effectiveness of sampling.

Following the UHF Gen 2 protocol, tags talk to the RFID reader with an anti-collision algorithm [22]. With the algorithm, multiple tags may respond to the reader simultaneously and send their RN16, but only one tag can be activated and send the EPC together with the low level data in every time slot. Fig. 1 shows the equivalent circuits of two tags with mutual coupling under two scenarios [23]. Here, V_1 and V_2 are the equivalent source voltages when Tag 1 and Tag 2 are activated, respectively; I_1 and I_2 are the equivalent source currents when Tag 1 and Tag 2 are activated, respectively; Z_{L1} and Z_{L2} are the chip impedances, and Z_{A1} and Z_{A2} are the antenna input impedances of Tag 1 and Tag 2, respectively. We have the following theorem.

Theorem 1. *When two tags have strong mutual coupling, if they have the same chip and antenna input impedances, i.e., $Z_{L1} = Z_{L2}$ and $Z_{A1} = Z_{A2}$, the ratio of their equivalent source currents equals to the ratio of their equivalent source voltages, i.e., $I_1/I_2 = V_1/V_2$.*

Proof: When Tag 1 is activated, the current I_1 in Tag 1 will produce a magnetic field, thus leading to a coupled voltage $V_{21} = Z_{21}I_1$ in Tag 2, where Z_{21} is the mutual impedance in Tag 2 because of Tag 1. This coupled voltage V_{21} in Tag 2 will induce a current I_2^m, which also causes a coupled voltage $V_{12} = Z_{12}I_2^m$. Then we have

$$\begin{cases} I_1(Z_{L1} + Z_{A1}) = V_1 + Z_{12}I_2^m \\ I_2^m(Z_{L2} + Z_{A2}) = Z_{21}I_1. \end{cases} \quad (3)$$

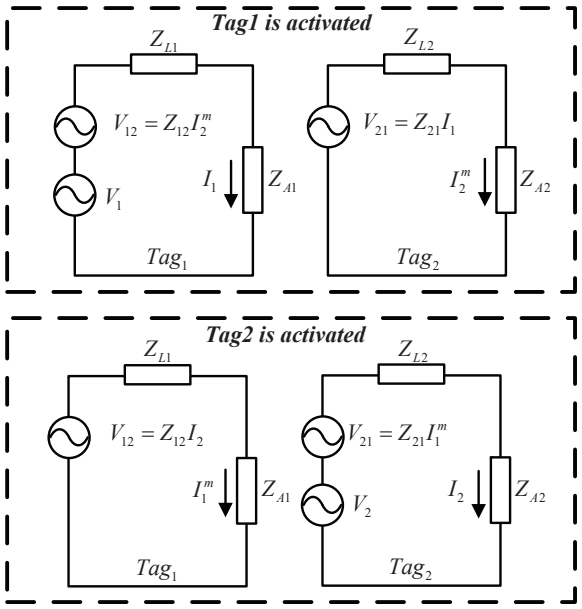

Fig. 1. Equivalent circuit of two tags with mutual coupling.

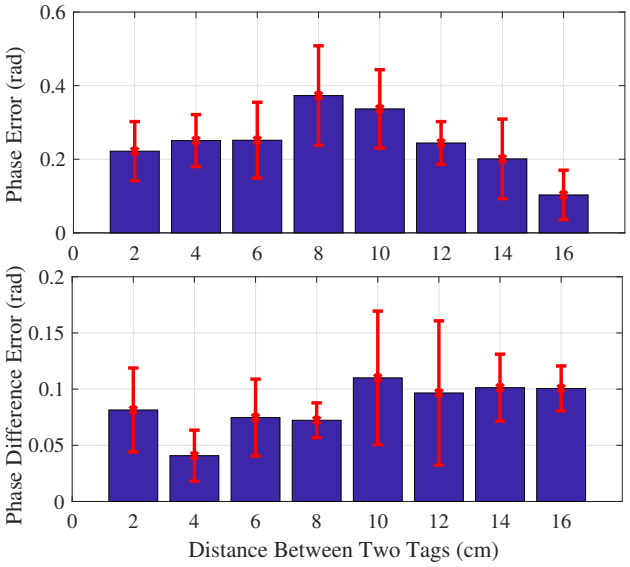

Fig. 2. Impact of mutual coupling on phase and phase difference.

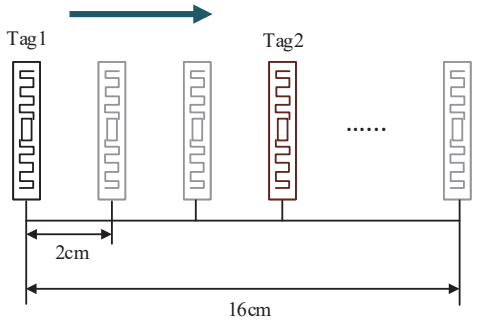

Fig. 3. Experiment scenario for impact of mutual coupling on phase difference.

For the same pair of tags, their mutual impedances are identical [23]. We use Z_m instead of Z_{12} or Z_{21} to simplify notation. The current I_1 in Tag 1 is

$$I_1 = \frac{V_1}{Z_0 - Z_m^2/Z_0}, \tag{4}$$

where $Z_0 = Z_{L1} + Z_{A1} = Z_{L2} + Z_{A2}$. Similarly, when Tag 2 is activated, we have the following equations.

$$\begin{cases} I_1^m(Z_{L1} + Z_{A1}) = Z_{12}I_2 \\ I_2(Z_{L2} + Z_{A2}) = V_2 + Z_{21}I_1^m, \end{cases} \tag{5}$$

where I_1^m is induced from the coupling voltage V_{12}. We derive the current I_2 in Tag 2 as

$$I_2 = \frac{V_2}{Z_0 - Z_m^2/Z_0}, \tag{6}$$

It follows that $I_1/I_2 = V_1/V_2$. ■

Define $I_i = |I_i|\angle I_i$ and $V_i = |V_i|\angle V_i$, $i = 1, 2$, where $|\cdot|$ denotes the amplitude and $\angle$ denotes the phase. It follows Theorem 1 that

$$\angle I_1 - \angle I_2 = \angle V_1 - \angle V_2. \tag{7}$$

Therefore, the phase difference between the currents of the two tags (i.e., $\angle I_1 - \angle I_2$) only depends on the phase difference between the source voltages of the two tags (i.e., $\angle V_1 - \angle V_2$), which is independent to the coupling voltage and mutual impedance. The measured phase at the RFID reader depends on the phase of the current that triggers the backscattered signal [24] (as well as the tag-reader distance). Thus the measured phase difference between the two tags is independent to the coupling voltage and mutual impedance. The impact of mutual coupling on the *measured phase difference* is thus limited. Note that as shown in (4) and (6), the currents I_1 and I_2 themselves are functions of the mutual impedance Z_m, so the *measured phase* itself is susceptible to the coupling effect.

To evaluate the impact of mutual coupling on measured phases and measured phase differences, we conduct the following two experiments to verify our analysis. In the *first* experiment, we measure the phase of a tag on a specific channel, while placing another tag next to it; the phase values under different coupling distances are collected. In the upper plot of Fig. 2, we plot the phase errors at different coupling distances. The ground truth is measured without the second tag (i.e., absence of the coupling effect). We find that the phase errors are all larger than 0.2 radians when the tag distance is smaller than 16 cm. Only when the distance is longer than 16 cm, the change of phase becomes lower than 0.1 radians. Thus, to avoid the coupling effect on measured phase, the distance of two adjacent tags must be larger than 16 cm.

In the *second* experiment, we evaluate the mutual coupling effect on measured phase difference, where two tags are placed on the same plane parallel to each other. As shown in Fig. 3, we first employ only a single tag. We put Tag 1 at each of the locations that are 2 cm apart, and measure the phase of the

tag at each location. Then we subtract the measured phase at the left-most position from the measured phases at all other locations, to obtain the ground truth of phase difference (under no coupling effect). Then, we put Tag 1 back to the left-most position, and put Tag 2 at each of the 2 cm apart positions. We then measure the phase difference between the two tags at various tag-to-tag distances from 2 cm to 16 cm. In the lower plot of Fig. 2, we present the phase difference errors (as compared to the ground truth) over tag distances. Because of multipath effect and thermal noise, there are still some error between ground truth and measured phase difference. However, we find most of the errors are lower than 0.1 radians, implying that *the phase difference of the two tags in the same plane is not heavily affected by mutual coupling. This experiment validates Theorem 1, which ensures the feasibility for using an RFID tag array for DOA estimation.*

Note that this experiment is different from Tagyro [12]. Tagyro is focused on the change of phase difference when one tag rotates around another fixed tag. Since the relative orientation between the two tags affects the mutual impedance, the mutual coupling effect will be different when the tag has different rotation angles. Thus, Tagyro requires phase difference calibration using a hologram based method to transform phase offset to orientation of the RFID tag array.

Consider a ULA tag array that has been interrogated by a reader for a period of time. In fact, the tags cannot be too close to each other, because the strong mutual coupling will make it harder for the reader to detect the tags. Through our extensive experiments, we find the tags closer to the center of the array are usually sampled by the reader at a lower rate. This is because the coupling effect caused by tags on both sides are very strong due to the short distance to the center tag. *To ensure that all tags in the array can transmit a sufficient amount of information to the reader, the density of the tag array cannot be too high. This motivates us to design a sparse RFID array.*

III. The SparseTag System

A. SparseTag System Design

As shown in Fig. 4, the SparseTag design employs an RFID tag array and two antennas (i.e., RFID readers), each of which can extract phase information from the 50 different frequencies used for channel hopping. The idea is to use the RFID tag array for determining the DOA between the center of the array and each antenna. Then, based on the two estimated DOA values and the known reader antenna positions, the center position of the RFID tag array can be accurately determined.

The main challenge of SparseTag is how to effectively estimate DOA values using a limited RFID tag array, which is attached on a small object (e.g., a book or an iPad). The traditional ULA design requires half of wavelength as the minimum distance between two tags, and usually the MUSIC algorithm is used for DOA estimation [20]. In fact, ULA is not proper for localizing a small object with an RFID tag array, because half of wavelength is approximately 16 cm already (the RFID reader operates from 902.5 MHz to 927.5 MHz).

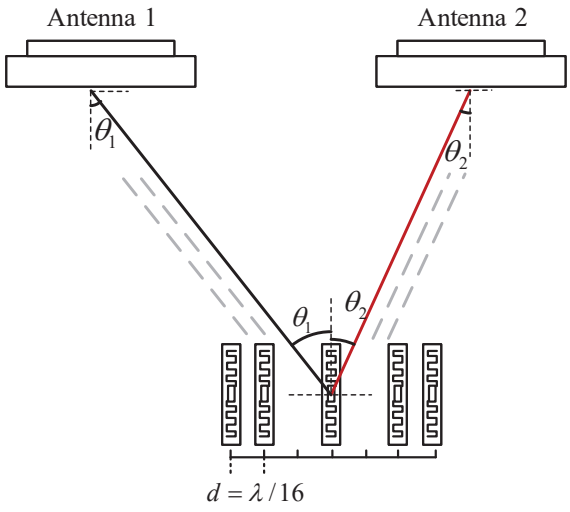

Fig. 4. The proposed SparseTag system with two readers and one sparse tag array.

Moreover, an N-element ULA with the traditional MUSIC method only estimates up to $(N-1)$ DOA values, and employs spatial smoothing for decorrelating uncorrelated sources. The maximum number of estimated DOA values will be halved. In this paper, *we propose a new sparse RFID tag array design to improve the success rate of sampling, where the minimum distance between two tags is only* $\lambda/16$. Since the width of a normal RFID tag is about 1cm, the minimum distance between two tags should be larger than 1 cm to avoid overlapping of tags. Thus we set the minimum distance between two tags in our array as $\lambda/16$, which is about 2cm. Furthermore, *we design the difference co-array for the sparse RFID tag array, which can obtain a higher DOA resolution with measured phase information.* The SparseTag system consists of four components: (i) Sparse Array Processing, (ii) Co-array Design, (iii) DOA Estimation, and (iv) Localization Method, which will be discussed in the following.

B. Sparse Array Processing

Since the number of tags should be limited (when positioning small objects), we will incorporate a sparse array for DOA estimation, with an N-element, nonuniform linear antenna array instead of a ULA with MUSIC [20]. Denote the steering vector for direction θ as $\vec{a}(\theta)$. The ith element of $\vec{a}(\theta)$ is $\exp\{j\frac{2\pi}{\lambda}d_i \sin\theta\}$, where d_i is the position of the ith tag and λ is the carrier wavelength. Consider D multipaths for the indoor environment, with directions θ_i and powers σ_i^2, $i = 1, 2, ..., D$, respectively. The received signal at time t is given by

$$\begin{aligned}\vec{g}[t] &= \sum_{i=1}^{D} \vec{a}(\theta_i)s_i[t] + \vec{n}[t] \\ &= \mathbf{A}\vec{s}[t] + \vec{n}[t],\end{aligned} \tag{8}$$

where $\mathbf{A} = [\vec{a}(\theta_1), \vec{a}(\theta_2), ..., \vec{a}(\theta_D)]$ denotes the array manifold matrix, $\vec{s}[t] = [s_1[t], s_2[t], ..., s_D[t]]^T$ is the source

signal vector, and $\vec{n}[t]$ is the white noise vector. Assume that the multipaths are temporally uncorrelated. Thus, the source autocorrelation matrix is diagonal. By leveraging the second order information of the received signal, we derive the covariance matrix of $\vec{g}(t)$ by

$$\begin{aligned}\mathbf{R}_{gg} &= \mathbb{E}[\vec{g}(t)\vec{g}(t)^H] \\ &= \mathbf{A}\mathbf{R}_{ss}\mathbf{A}^H + \sigma_n^2\mathbf{I} \\ &= \sum_{i=1}^{D}\sigma_i^2\vec{a}(\theta_i)\vec{a}(\theta_i)^H + \sigma_n^2\mathbf{I}.\end{aligned} \tag{9}$$

Then, by vectoring matrix $\mathbf{R}_{gg}$, we obtain the measurement vector as the following.

$$\begin{aligned}\vec{z} &= \text{vec}(\mathbf{R}_{gg}) \\ &= \text{vec}\left[\sum_{i=1}^{D}\sigma_i^2\vec{a}(\theta_i)\vec{a}(\theta_i)^H\right] + \sigma_n^2\vec{1}_n \\ &= (\mathbf{A}^* \odot \mathbf{A})\vec{p} + \sigma_n^2\vec{1}_n,\end{aligned} \tag{10}$$

where $\vec{p} = [\sigma_1^2, \sigma_2^2, ..., \sigma_D^2]^T$, $\vec{1}_n = [\vec{e}_1^T, \vec{e}_2^T, ..., \vec{e}_N^T]^T$, and $\vec{e}_i$ is a column vector with 1 at the ith position and 0 at all other positions. Note that $\vec{z}$ is considered as the signal received at an array with a manifold given by $(\mathbf{A}^* \odot \mathbf{A})$ [25], where $\odot$ denotes the Khatri-Rao (KR) product. Matrix $(\mathbf{A}^* \odot \mathbf{A})$ can be considered as the manifold of a longer array whose antenna positions are provided by the different values in set $\vec{x}_i - \vec{x}_j, 1 \le i, j \le N$, where $\vec{x}_i$ denotes the location vector of the ith tag of the array. This new array is called the *difference co-array* [25]. We perform DOA estimation using the difference co-array instead of the traditional array, which can exploit the second-order statistics of the received RFID signal to effectively increase the DOF.

C. Difference Co-array Design

1) Definitions:

Definition 1. *(Difference Co-Array). Consider a sparse N-element RFID tag array and let $\vec{x}_i$ denote the location vector of the ith tag. The difference co-array is defined as [25]*

$$\mathcal{D} = \{\vec{x}_i - \vec{x}_j, 1 \le i, j \le N\}. \tag{11}$$

The difference co-array can be considered as a new array where RFID tags are put at the locations in set $\mathcal{D}$. Moreover, the different values of the cross correlation terms in the covariance matrix of the received signal by the sparse RFID tag array can be determined by the number of elements in the difference co-array, which helps to increase the number of estimated DOAs.

Definition 2. *(Restricted Array). A sparse N-element RFID tag array is a restricted array if its difference co-array is hole-free [26].*

If the difference co-array is hole-free, it is also a ULA. Thus, the traditional subspace based MUSIC algorithm can be used for DOA estimation with a hole-free difference co-array. For example, if the tags are deployed at locations that are given by set S, as

$$\mathcal{S} = \{md, m = 1, 2, 4\}. \tag{12}$$

where d is the minimum distance between two adjacent tags. Its difference co-array can be calculated as

$$\mathcal{D} = \left\{-\vec{3}, -\vec{2}, -\vec{1}, \vec{0}, \vec{1}, \vec{2}, \vec{3}\right\}. \tag{13}$$

although the $3d$ position is missing in the example sparse array, there is no missing vector in the difference co-array set $\mathcal{D}$ (i.e, including all the vectors from $-\vec{3}$ to $\vec{3}$), which means the array is still suitable for the MUSIC algorithm.

Definition 3. *(Degree of Freedom): The DOF of a sparse RFID array is the cardinality of its difference co-array $\mathcal{D}$ [25].*

The DOF of a sparse RFID array can be computed by the cardinality of its difference co-array $\mathcal{D}$, which indicates the maximum number of estimated DOAs.

Definition 4. *(Weight Function). For a sparse N-element RFID tag array, its weight function $w(\vec{d})$ is the number of tag pairs that can achieve the difference co-array element $\vec{d}$. The weight function is defined as [25]*

$$w(\vec{d}) = \left|\left\{(\vec{x}_i, \vec{x}_j) | \vec{x}_i - \vec{x}_j = \vec{d}\right\}\right|, \vec{d} \in \mathcal{D}. \tag{14}$$

The weight function measures the strength of mutual coupling, which is helpful for our sparse RFID tag array.

2) Design of Difference Co-array: For a fixed N-element sparse RFID tag array (N is an odd number), the tag locations are given by set S, as

$$\begin{aligned}\mathcal{S} = \{&md, m = 1, ..., (N+1)/2 - 1, \\ &(N+1)/2 + 1, (N+1)/2 + 3, ..., N+2\}.\end{aligned} \tag{15}$$

where the minimum distance is set to $d = \lambda/16$, which enables the use of a small-sized RFID tag array. Note that the proposed sparse RFID tag array has a symmetric structure, where the left and right sections have the same space separate with d. Moreover, the distance from the two tags at $(\frac{N+1}{2} - 1)d$ and $(\frac{N+1}{2} + 3)d$ to the center tag (at location $\frac{N+3}{2}d$) is both $2d$, which causes the sparseness of the proposed array.

The design of the sparse RFID tag array has three key features. First, because of the symmetric structure, strong mutual coupling typically found in small RFID tag arrays can now be greatly reduced, thus enabling accurate DOA estimation. Second, a smaller sparse RFID tag array can avoid the reduction of sampling rate of the center tag, because the three middle tags are separated at a larger distance $2d$. Third, a smaller sparse RFID tag array can improve the DOA resolution and is easy to attach to small objects.

The difference co-array of the proposed sparse RFID tag array can be obtained by the following position set S_d, as

$$\mathcal{S}_d = \{md, m = -(N+1), ..., (N+1)\}. \tag{16}$$

We have the following theorems for the difference co-array of the sparse RFID tag array.

Theorem 2. *The proposed sparse RFID tag array is a restricted array, i.e., it is a hole-free difference co-array.*

Proof: The difference co-array of the proposed sparse RFID array is an ULA, which is a hole-free difference co-array based on the position set $\mathcal{S}_d$. Therefore, it is a restricted array. This proofs the theorem. ■

Corollary 2.1. *The proposed sparse RFID array has the same co-array as an* $(N+2)$ *ULA.*

Proof: First, the proposed sparse RFID array has the same boundary positions at d and $(N+2)d$ as an $(N+2)$ ULA. Moreover, these two arrays are both restricted arrays. Thus, the proposed sparse RFID tag array has the same co-array as the $(N+2)$ ULA. ■

Theorem 3. *The DOF of the sparse* N*-element RFID tag array is* $2N+3$.

Proof: For the proposed sparse RFID array with set $\mathcal{S}$, the cardinality of its difference co-array $\mathcal{S}_d$ is $2N+3$. Thus, its DOF is $2N+3$ according to Definition 3. ■

Theorem 4. *For the sparse* N*-element RFID tag array, its weight function* $w(\vec{d}=\vec{0})=N$*, and* $w(\vec{d}=\vec{1})=N-3$.

Proof: The case $\vec{d}=\vec{0}$ occurs if $\vec{x}_i=\vec{x}_j$. For an N-element array, this case occurs N times, when $i=j=1,2,...,N$. Thus $w(\vec{d}=\vec{0})=N$.

On the other hand, consider two different subarrays with position sets $\mathcal{S}_l=\{md, m=1,...,\frac{N+1}{2}-1\}$ and $\mathcal{S}_r=\{md, m=\frac{N+1}{2}+3,...,N+2\}$. The case $\vec{d}=\vec{1}$ occurs $\frac{N+1}{2}-2$ times in each subarray. Moreover, for the subarray with position set $\mathcal{S}_c=\{md, m=\frac{N+1}{2}-1, \frac{N+1}{2}+1, \frac{N+1}{2}+3\}$, the case $\vec{d}=\vec{1}$ does not occur at all. Thus we have $w(\vec{d}=\vec{1})=(\frac{N+1}{2}-2)*2=N-3$. This proofs the theorem. ■

Based on the above theorems, we conclude that

- The N-element sparse RFID tag array has the same DOF as an $(N+2)$-element ULA. The maximum number of estimated DOAs can be improved by using the proposed sparse array, compared with the ULA with the same number of tags using the subspace-based MUSIC method.
- Because the proposed sparse array has a smaller $w(\vec{d}=\vec{1})=N-3$ than the $(N+2)$-element ULA, the proposed array can achieve a higher sampling rate.

  Figs. 5 and 6 present a seven-tag ULA and its weight function, and a five-tag sparse array and its weight function, respectively. We can see that the five-tag sparse array has the same DOF of 13 as the seven-tag ULA, because they have the same difference co-array. Moreover, it can be seen that $w(\vec{1})=2$ for the five-tag sparse array, while $w(\vec{1})=6$ for the seven-tag ULA.
- Although other sparse arrays, such as co-prime array [27], nested array [25], and super nested array [28], can achieve larger DOFs than the proposed array, these arrays are not proper for RFID deployment for two reasons. First, these arrays require a larger space, which is not suitable for localizing small objects. Second, these arrays do not have a symmetric structure. Thus, they suffer from stronger mutual coupling effects, which usually cause larger DOA estimation errors.

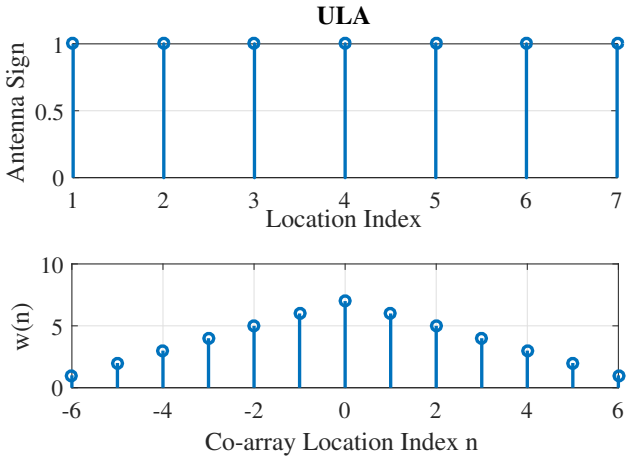

Fig. 5. A 7-tag ULA and its weight function. Antenna sign is 1 means a tag will be placed at the corresponding location.

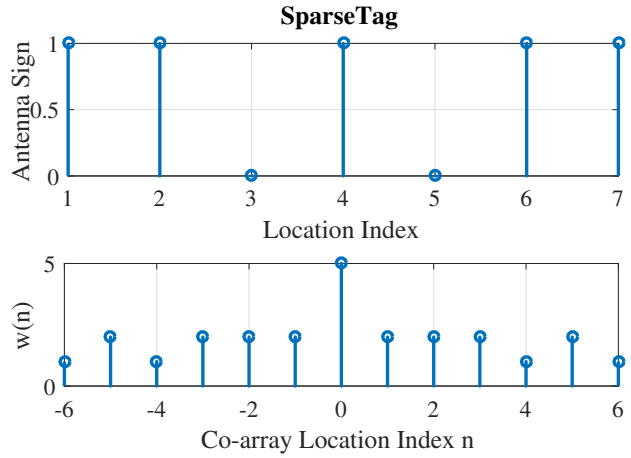

Fig. 6. A 5-tag sparse array and its weight function. Antenna sign is 1 means a tag will be placed at the corresponding location

D. DOA Estimation

We next estimate DOA with the difference co-array of the proposed sparse RFID tag array, employing a spatial smoothing based method. This is different from the traditional spatial smoothing base approach for mitigating correlated sources [25]. This technique creates an observation matrix for the difference co-array, and thus avoids the use of the high-order cumulative signal.

From (10), we obtain the new array manifold $(\mathbf{A}^* \odot \mathbf{A})$ with dimension $N^2 \times D$. Recall that the DOF of the proposed difference co-array is $2N+3$. Thus, we can create a new matrix $\mathbf{B}$ of dimension $(2N+3)\times D$ by removing the repeated rows in the array manifold $(\mathbf{A}^* \odot \mathbf{A})$. Then, we sort the new matrix so that the ith row corresponds to the RFID tag position $(-N-1+i)d$ in the proposed difference co-array. We obtain

a new vector $\vec{y}$, which is given by

$$\vec{y} = \mathbf{B}\vec{p} + \sigma_n^2 \vec{e}, \tag{17}$$

where $\vec{e} \in \Re^{(2N+3)\times 1}$ is a vector of all zeros except a single 1 at the $(N+1)$th position.

According to (16), we separate the co-array into $(N+1)$ overlapping subarrays, each of which has $(N+1)$ elements. The ith subarray is deployed at the following position set:

$$\mathcal{S}_i = \{(-i+1+m)d,\ m = 0, 1, ..., N\}. \tag{18}$$

We define $\vec{y}_i$ as a new vector for the ith subarray, which consists of elements of $\vec{y}$ from the $(N+1-i+1)$th to the $(2N+1-i+1)$th position. The vector $\vec{y}_i$ is given by

$$\vec{y}_i = \mathbf{B}_i\vec{p} + \sigma_n^2 \vec{e}^i, \tag{19}$$

where $\mathbf{B}_i$ is a $(N+1)\times D$ matrix, which consists of the $(N+1-i+1)$th to the $(2N+1-i+1)$th rows of $\mathbf{B}$ and $\vec{e}^i$ is a vector of all zeros except a single 1 at the ith position.

Next, we obtain the spatially smoothed matrix $\mathbf{R}_s$, given by

$$\mathbf{R}_s = \frac{1}{N+1}\sum_{i=1}^{N+1} \vec{y}_i \vec{y}_i^H. \tag{20}$$

Finally, we implement DOA estimation based on matrix $\mathbf{R}_s$. The maximum number of estimated DOAs is N, which is larger than the MUSIC based ULA approach using spatial smoothing (for which the maximum number of estimated DOAs is $(N-1)/2$). In the SparseTag design, we use a directional antenna to increase the transmission range. Thus, LOS is the dominant component of the wireless channel, which leads to a strong incoming wave. The proposed RFID tag array can achieve a higher angle resolution than the traditional MUSIC method.

E. Localization Estimation

The SparseTag system consists of an RFID tag array and two reader antennas, each of which can extract phase information from each of the 50 channels. In indoor environments, not all channel information are reliable because of the multipath effect. To this end, we propose a robust channel selection method based on the sparse RFID tag array.

Let $\varphi_{(i,f_m)}(t)$ denote the phase value from tag i on frequency f_m at time t. The phase difference $\Delta_{(i,f_m)}(t)$ between tag i and tag $i+1$ is

$$\Delta_{(i,f_m)}(t) = \varphi_{(i+1,f_m)}(t) - \varphi_{(i,f_m)}(t), i = 1, ..., N-1. \tag{21}$$

Among the phase difference values $\Delta_{(i,f_m)}(t)$ of all frequencies, we select the medium value for improved robustness, because usually only a few channels are corrupted by the multipath effect. After channel selection, we recompute the phase values for all tags. Setting the phase of Tag 1 $\varphi_{(1,f_m)}(t) = 0$ at time t, the phase value of Tag i is

$$\varphi_{(i,f_m)}(t) = \varphi_{(i-1,f_m)}(t) + \Delta_{(i-1,f_m)}(t), i = 2, ..., N. \tag{22}$$

We next reconstruct the received signal, as

$$\hat{g}(t) = [e^{(j(2\pi - \varphi_{(1,f_m)}(t)))}, ..., e^{(j(2\pi - \varphi_{(N,f_m)}(t)))}]. \tag{23}$$

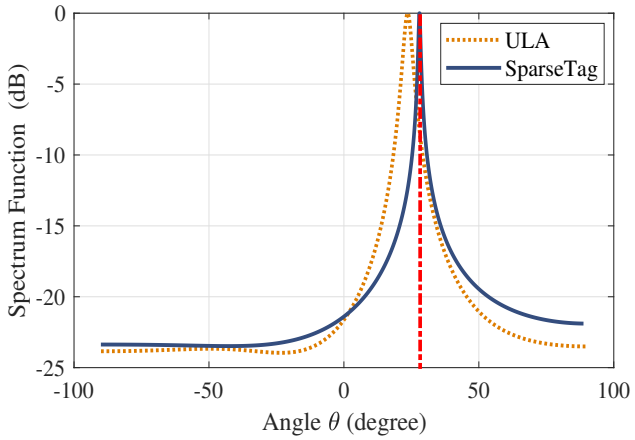

Fig. 7. Angle estimation results using ULA and SparseTag.

Here we use $2\pi - \varphi_{(1,f_m)}(t)$ because of the RFID reader phase operation. Using the received signal from multiple snapshots (each consisting of samples from the 50 channels), we can estimate two DOA values using the proposed method with the sparse RFID tag array. Fig. 7 presents the power spectrum function calculated for SparseTag and ULA arrays at the same position. The ground truth DOA is marked by the red line, which is 28°. From Fig. 7, we observe that the peak of SparseTag is much sharper and closer to the ground truth than that of ULA with MUSIC. The DOA estimation based on SparseTag is more accurate than ULA, because SparseTag achieves a larger number of DOFs than ULA.

Once the two DOA values are estimated, we can leverage them for locating the RFID tag array. Let the tag array be the x-axis, and the y-axis be perpendicular to the tag array. Let (x_i, y_i) denote the position of RFID reader i, $i = 1, 2$, and (x_c, y_c) denote the center position of the tag array. The two DOA values satisfy

$$\begin{cases} \cot(\theta_1) = \frac{y_c - y_1}{x_c - x_1} \\ \cot(\theta_2) = \frac{y_c - y_2}{x_c - x_2}, \end{cases} \tag{24}$$

where the cotangent function is defined as $\cot(\theta) = \cos(\theta)/\sin(\theta)$. Solving the two equations in (24), the center position of the RFID tag array can be computed as

$$x_c = \frac{x_1\cot(\theta_1) - x_2\cot(\theta_2) + y_2 - y_1}{\cot(\theta_1) - \cot(\theta_2)} \tag{25}$$

$$y_c = \frac{(x1 - x2)\cot(\theta_1)\cot(\theta_2) + y_2\cot(\theta_1) - y_1\cot(\theta_2)}{\cot(\theta_1) - \cot(\theta_2)}. \tag{26}$$

IV. Experimental Study

A. Experiment Configuration

To evaluate the performance of SparseTag, we develop a prototype with an off-the-shelf Impinj R420 RFID reader equipped with two circular polarized antennas. The channel used to scan RFID tags automatically hops among 50 channels from 902.5 MHz to 927.5 MHz, which is FCC-compliant. A Lenovo Thinkpad S3 laptop is used as a user interface and

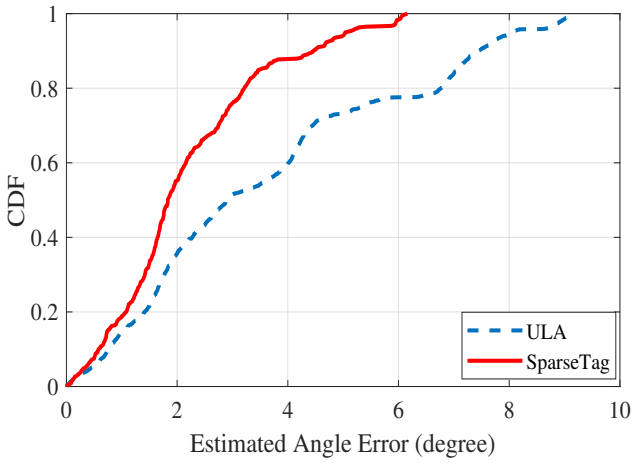

Fig. 8. CDFs of angle errors using a 5-tag SparseTag and a 5-tag ULA in the computer lab experiment.

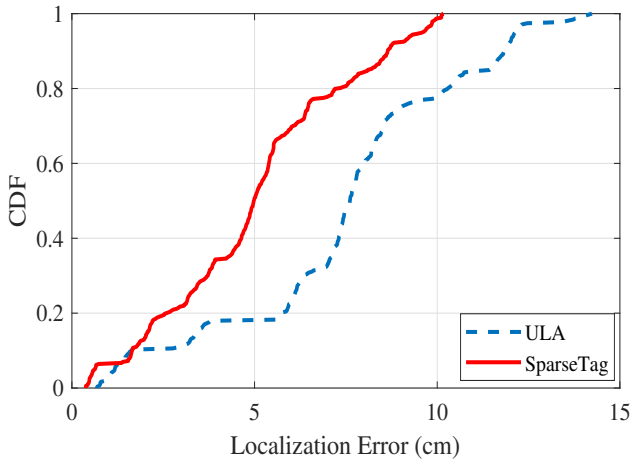

Fig. 9. CDFs of localization errors using a 5-tag SparseTag and a 5-tag ULA in the computer lab experiment.

for signal processing. The software used in our experiment is based on an RFID library, which allows the computer to communicate with the RFID reader. The RFID reader can extract data from tags, including time stamp, phase angle, RSSI, and Doppler shift based on a Low-level Reader Protocol (LLRP). Moreover, we create RFID tag arrays using three different types of RFID tags, including ALN-9740, SMARTRAC DogBone, and SMARTRAC ShortDipole.

We test the SparseTag system in a 7.5m $\times$ 5.6m computer laboratory and an 8m $\times$ 2.4m anechoic chamber. The computer laboratory is crowded with computers, desks, and chairs, which can cause considerable multipath effect. In the anechoic chamber, most multipath effect can be removed with the special material mounted on the wall, ceiling, and floor. We set up the coordinates for antennas and calculate the center position of the sparse RFID tag array based on estimated angle by each reader antenna.

B. Performance of Tag Localization

Fig. 8 presents a comparison of SparseTag with ULA in the computer lab environment. The cumulative distribution function (CDF) of angle errors for a 5-tag ULA and a 5-tag SparseTag are plotted. For the 5-tag ULA, we use MUSIC for DOA estimation [13], [20]. We can see the maximum estimated angle error for ULA is $9.198°$, while the maximum angle error for SparseTag is $6.161°$. The median errors for ULA and SparseTag are $2.909°$ and $1.831°$, respectively. Furthermore, 90% of estimated angle errors by SparseTag are less than $5°$. We conclude that SparseTag is more accurate on angle estimation than ULA, because SparseTag achieves a higher angle resolutions than ULA.

Fig. 9 shows the CDF of localization errors for the 5-tag ULA and 5-tag SparseTag. We employ the same localization method on two different tag arrays in the same environment. We observe that the median error for SparseTag is 4.985 cm, while the median error of ULA is 7.611 cm. From Fig. 9, it can be seen that the maximum error of SparseTag is 10.114 cm, which is much smaller than that of ULA. SparseTag can achieve higher accuracy of localization than that of ULA. Since our localization method is based on angle estimation with two antennas, higher angle estimation accuracy will directly lead to more accurate localization estimation.

Fig. 10 and Fig. 11 are the 5-tag SparseTag results in the computer lab and anechoic chamber environments. The CDFs of angle errors and localization errors are plotted, respectively. We can see that the median error of angle estimation in the anechoic chamber is $1.125°$, while the median error in the computer laboratory is $1.872°$. Fig. 10 also shows that the maximum error in anechoic chamber is only $4.024°$. The angle estimation accuracy is much higher when the system is tested in the anechoic chamber, because the multipath effect is eliminated in the anechoic chamber environment. From Fig. 11, we also observe that the location error in the anechoic chamber is smaller than that in the computer laboratory environment. The median location error in the anechoic chamber environment is 3.419 cm, while the median location error in the computer lab environment is 5.012 cm.

V. Conclusions

In this paper, we proposed SparseTag, a sparse RFID tag array system for high accuracy backscatter indoor localization. We designed the SparseTag system, which includes sparse array processing, difference co-array design, DOA estimation using a spatial smoothing based method, and a DOA-based localization method. To mitigate the multipath effect, we proposed a robust channel selection method. We prototyped the SparseTag system with commercial RFID tags and reader, and evaluated its performance in two indoor environments. The experimental results validated the effectiveness and location accuracy of the proposed SparseTag system.

Acknowledgment

This work is supported in part by the US NSF under Grant CNS-1702957, and through the Wireless Engineering Research and Education Center (WEREC) at Auburn University. Any

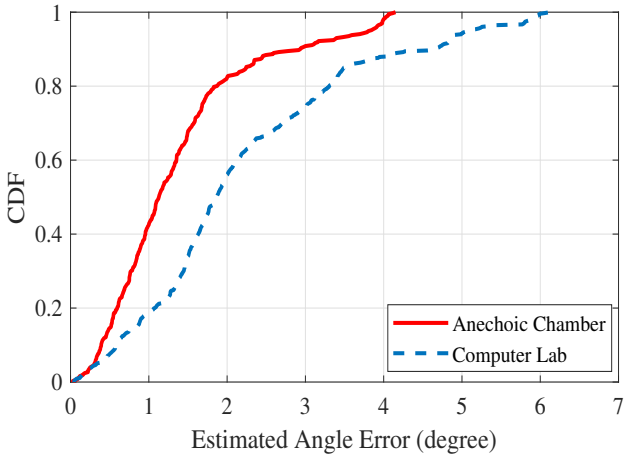

Fig. 10. CDFs of angle errors achieved by the 5-tag SparseTag in the computer laboratory and anechoic chamber scenarios.

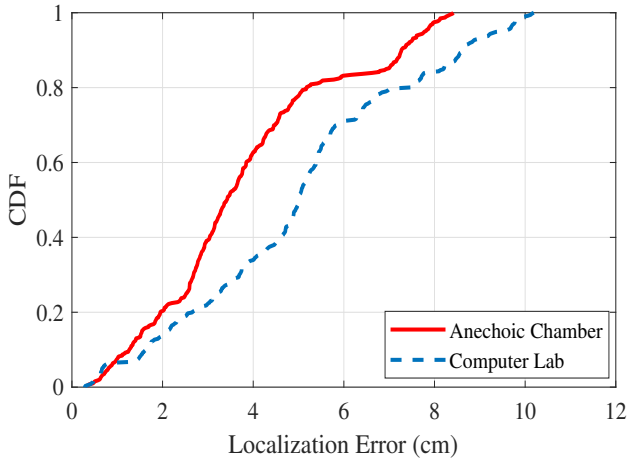

Fig. 11. CDFs of localization errors achieved by the 5-tag SparseTag in the computer laboratory and anechoic chamber scenarios.

opinions, findings, and conclusions or recommendations expressed in this material are those of the authors and do not necessarily reflect the views of the foundation.

REFERENCES

[1] C. Yang, X. Wang, and S. Mao, "AutoTag: Recurrent vibrational autoencoder for unsupervised apnea detection with RFID tags," in *Proc. IEEE GLOBECOM 2018*, Abu Dhabi, UAE, Dec. 2018, pp. 1–7.

[2] X. Wang, J. Zhang, Z. Yu, E. Mao, S. Periaswamy, and J. Patton, "RF Thermometer: A temperature estimation method with commercial UHF RFID tags," in *Proc. IEEE ICC 2019*, Shanghai, China, May 2019, pp. 1–6.

[3] J. Zhang, Z. Yu, X. Wang, Y. Lyu, S. Mao, S. C. Periaswamy, J. Patton, and X. Wang, "RFHUI: An intuitive and easy-to-operate human-uav interaction system for controlling a UAV in a 3D space," in *Proc. EAI MobiQuitous 2018*, New York City, NY, Nov. 2018, pp. 69–76.

[4] J. Zhang, Z. Yu, X. Wang, Y. Lyu, S. Mao, S. Periaswamy, J. Patton, and X. Wang, "RFHUI: An RFID based human-unmanned aerial vehicle interaction system in an indoor environment," *Elsevier Digital Communications and Networks Journal*, to appear.

[5] L. M. Ni, Y. Liu, Y. C. Lau, and A. P. Patil, "LANDMARC: Indoor location sensing using active RFID," in *Proc. IEEE PerCom 2003*, Dallas, TX, Mar. 2003, pp. 407–415.

[6] J. Wang, D. Vasisht, and D. Katabi, "RF-IDraw: Virtual touch screen in the air using RF signals," in *ACM SIGCOMM Comput. Commun. Rev.*, vol. 44, no. 4, Oct. 2014, pp. 235–246.

[7] J. Wang and D. Katabi, "Dude, where's my card? RFID positioning that works with multipath and non-line of sight," in *ACM SIGCOMM Comput. Commun. Rev.*, vol. 43, no. 4, Oct. 2013, pp. 51–62.

[8] L. Yang, Y. Chen, X.-Y. Li, C. Xiao, M. Li, and Y. Liu, "Tagoram: Real-time tracking of mobile RFID tags to high precision using COTS devices," in *Proc. ACM MobiCom'14*, Maui, HI, Sept. 2014, pp. 237–248.

[9] L. Shangguan and K. Jamieson, "The design and implementation of a mobile RFID tag sorting robot," in *Proc. ACM MobiSys'16*, Singapore, June 2016, pp. 31–42.

[10] T. Liu, L. Yang, Q. Lin, Y. Guo, and Y. Liu, "Anchor-free backscatter positioning for RFID tags with high accuracy," in *Proc. IEEE INFOCOM'14*, Toronto, Canada, Apr./May 2014, pp. 379–387.

[11] Y. Zhang, M. G. Amin, and S. Kaushik, "Localization and tracking of passive rfid tags based on direction estimation," *International Journal of Antennas and Propagation*, vol. 2007, 2007.

[12] T. Wei and X. Zhang, "Gyro in the air: tracking 3d orientation of battery-less internet-of-things," in *Proceedings of the 22nd Annual International Conference on Mobile Computing and Networking*. ACM, 2016, pp. 55–68.

[13] H. Jin, Z. Yang, S. Kumar, and J. I. Hong, "Towards wearable everyday body-frame tracking using passive RFIDs," *Proc. ACM on Interactive, Mobile, Wearable and Ubiquitous Technol.*, vol. 1, no. 4, p. No. 145, Dec. 2018.

[14] Y. Bu, L. Xie, J. Liu, B. He, Y. Gong, and S. Lu, "3-Dimensional reconstruction on tagged packages via RFID systems," in *Proc. IEEE SECON'17*, San Diego, CA, June 2017, pp. 1–9.

[15] Y. Zhang, L. Xie, Y. Bu, Y. Wang, J. Wu, and S. Lu, "3-Dimensional localization via RFID tag array," in *Proc. IEEE MASS'17*, Orlando, FL, Oct. 2017, pp. 353–361.

[16] F. Guidi, N. Decarli, S. Bartoletti, A. Conti, and D. Dardari, "Detection of multiple tags based on impulsive backscattered signals," *IEEE Transactions on Communications*, vol. 62, no. 11, pp. 3918–3930, 2014.

[17] M. Bolic, M. Rostamian, and P. M. Djuric, "Proximity detection with rfid: A step toward the internet of things," *IEEE Pervasive Computing*, vol. 14, no. 2, pp. 70–76, 2015.

[18] H. Ding, J. Han, C. Qian, F. Xiao, G. Wang, N. Yang, W. Xi, and J. Xiao, "Trio: Utilizing tag interference for refined localization of passive RFID," in *Proc. IEEE INFOCOM'18*, Honolulu, HI, Apr. 2018.

[19] F. Xiao, Z. Wang, N. Ye, R. Wang, and X.-Y. Li, "One more tag enables fine-grained RFID localization and tracking," *IEEE/ACM Trans. Netw.*, vol. 26, no. 1, pp. 161–174, Jan. 2018.

[20] R. Schmidt, "Multiple emitter location and signal parameter estimation," *IEEE Trans. Antennas Propag.*, vol. 34, no. 3, pp. 276–280, Mar. 1986.

[21] Impinj Support Portal, "Low level user data support," 2013, Impinj Speedway Revolution Reader Application, [online] Available: https://support.impinj.com.

[22] D. M. Dobkin, *The rf in RFID: UHF RFID in practice*. Newnes, 2012.

[23] F. Lu, X. Chen, and T. Y. Terry, "Performance analysis of stacked RFID tags," in *Proc. 2009 IEEE International Conference on RFID*, Orlando, FL, Apr. 2009, pp. 330–337.

[24] S. Pradhan, E. Chai, K. Sundaresan, L. Qiu, M. A. Khojastepour, and S. Rangarajan, "Rio: A pervasive RFID-based touch gesture interface," in *Proc. ACM MobiCom'17*, Snowbird, UT, Oct. 2017, pp. 261–274.

[25] P. Pal and P. Vaidyanathan, "Nested arrays: A novel approach to array processing with enhanced degrees of freedom," *IEEE Trans. Signal Process.*, vol. 58, no. 8, pp. 4167–4181, Aug. 2010.

[26] A. Moffet, "Minimum-redundancy linear arrays," *IEEE Trans. Antennas Propag.*, vol. 16, no. 2, pp. 172–175, Mar. 1968.

[27] P. P. Vaidyanathan and P. Pal, "Sparse sensing with co-prime samplers and arrays," *IEEE Trans. Signal Process.*, vol. 59, no. 2, pp. 573–586, Feb. 2011.

[28] C.-L. Liu and P. Vaidyanathan, "Super nested arrays: Linear sparse arrays with reduced mutual coupling–Part I: Fundamentals," *IEEE Trans. Signal Process.*, vol. 64, no. 15, pp. 3997–4012, Aug. 2016.